J. Chem. Soc., Faraday Trans. 1, 1983, **79**, 15-26

Kinetics of Monticular Carbon Growth on Polycrystalline Iron

BY ALAN M. EMSLEY AND MALCOLM P. HILL*

Central Electricity Research Laboratories, Kelvin Avenue, Leatherhead, Surrey KT22 7SE

Received 28th September, 1981

The kinetics of carbon deposition on polycrystalline iron surfaces from methane at 750 Torr† pressure and at temperatures between 1013 and 1133 K have been studied using the change in power dissipation of an electrically heated filament caused by the increased emissivity as the surface is blackened by deposit. The carbon formed has a monticular-type structure. The growth kinetics follow a direct logarithmic rate law which is explained in terms of the availability of active sites at the surface. The total carbon uptake at maximum coverage of the monticular layer, *i.e.* at maximum emissivity, depends on the filament temperature and can be correlated with the amount of carbon taken up into solution during the prior induction period in accordance with the phase diagram. The activation energy has a value of 66 ± 8 kJ mol^{-1}. The rate-determining step for monticular growth cannot be established, but certain possibilities, such as carbon dissolution, bulk diffusion of carbon in the metal, and surface and bulk self-diffusion of iron, can be eliminated. Various aspects of the mechanism of formation of the monticular growths are discussed.

The carbon deposits formed on iron by pyrolysis of hydrocarbons have a number of characteristic morphologies, including laminar graphitic layers, mound-type (monticular) growths, columnar morphology and filamentary material.[1-3] The deposit morphology, particularly in the early stages of reaction, depends on the metallurgical state of the substrate and therefore on its previous mechanical, thermal and chemical treatment.[4] The monticular type deposits are formed on specimens that have received insufficient heat treatment to remove the cold-worked layer at the metal surface. They can also be formed by diffusing carbon down a thermal gradient in a well annealed metal such that precipitation occurs where the temperature falls below that of the Fe–C eutectoid (996 or 1011 K).[5] As a phase change occurs at this transition, *i.e.* γ-(f.c.c.) Fe to α-(b.c.c.) Fe, it is possible that the monticular growths are associated with structural rearrangements of the metal surface. The surface of the mound is decorated with a polygonised ridge structure typical of the continuous laminar graphitic films formed in other transition-metal hydrocarbon systems.[6-8]

Two mechanisms have been proposed to explain the good graphitic order of the deposits, *viz.* (i) dissolution of carbon, nucleation at suitable sites, followed by precipitation, and (ii) formation and decomposition of an intermediate carbide.[9] Both surface and bulk diffusion mechanisms have been invoked to explain the development of particular morphologies.[10, 11] As yet there is no definite confirmation of any of these mechanisms.

After the carbon dissolution stage of the reaction is complete, precipitation of carbon and/or carbide can occur both at the surface and in the bulk metal.[12] To simplify the kinetics it is necessary to distinguish between bulk and surface processes, and a novel method of doing so has been adopted. The localised nature of surface deposit causes areas of high emissivity to be formed on the bright metal. The early

† 1 Torr = 101 325/760 Pa.

stages of deposit growth can be followed by measuring changes in the electrical power dissipation of the specimen. Resistivity measurements indicate when precipitation becomes significant in the bulk metal, and the reaction can be stopped before there is any interference with the surface measurements. We have used the technique with iron foils that have a retained cold-worked layer and therefore initially form only the monticular type of deposit. The morphology present at the reaction temperatures has been confirmed by separate *in situ* hot-stage scanning electron microscopy (SEM)[5] as well as conventional SEM examination after cooling. The formation of laminar carbon films on well annealed surfaces at temperatures above the Fe–C eutectoid is too rapid to follow by this technique.

THEORY

The power dissipation, $W(t)$, from an electrically heated foil is given by Stefan's law. For a surface with areas of differing emissivity, for example composed of bright metal with emissivity ε_M or carbon covered with emissivity ε_c:

$$W(t) = \sigma(T^4 - T_0^4)\{\varepsilon_M[a_g - a_p(t)] + \varepsilon_c a_p(t)\} + c \tag{1}$$

where σ is Stefan's constant, a_g the geometric area of the foil, $a_p(t)$ the projected area of a carbon mound on the surface, T the reaction temperature in K, T_0 the ambient temperature in K and c a constant which corrects for conduction losses at leads and convection losses. It is assumed that the actual carbon surface area, at a time t, $a_c(t)$, bears a constant relationship to its projected area $a_p(t)$, regardless of its detailed morphology, *i.e.*

$$\frac{a_c(t)}{a_p(t)} = A.$$

For a simple case of a solid hemispherical growth we have $A = 0.5$. In practice the morphology is complex and A cannot be defined. However, the assumption is valid for the early stages of growth, when the deposit is very thin. The bright metal emissivity remains constant during the experiment.

In the course of an experiment the change in power dissipation is given by

$$\Delta W(t) = \sigma(T^4 - T_0^4)\left[\varepsilon_M\left(a_g - \frac{a_c(t)}{A}\right) + \varepsilon_c a_c(t)\right] - \sigma(T^4 - T_0^4) a_g \varepsilon_M \tag{2}$$

$$= \sigma(T^4 - T_0^4)\left[a_c(t)\left(\varepsilon_c - \frac{\varepsilon_M}{A}\right)\right]. \tag{3}$$

In the early part of the deposition reaction the rate of carbon growth is proportional to the rate of increase of the high-emissivity area $da_c(t)/dt$, which is given by

$$\frac{da_c(t)}{dt} = \frac{d[\Delta W(t)]}{dt}\left(\frac{1}{\sigma(T^4 - T_0^4)\left(\varepsilon_c - \frac{\varepsilon_M}{A}\right)}\right). \tag{4}$$

Heat losses by conduction and convection are constant throughout the experiment and therefore do not enter into the final expression. The value of T_0 is assumed to remain constant over the narrow temperature range of the experiment, and will be slightly above ambient temperature because of wall heating.

The resistivity of the specimen increases during the later stages of the reaction because of localised carburisation. The power dissipation must be corrected for any such resistance increase. Eventually 'hot spots' will develop in these regions, but before they can influence the results the experiments are stopped.

EXPERIMENTAL

APPARATUS AND MATERIALS

The specimen consisted of a pure iron foil (99.99% pure, *ex.* Johnson–Matthey) 150 mm long, 1 mm wide and 0.025 mm thick, to which were spot-welded two 0.075 mm diameter Pt–Pt/Rh thermocouples (Thermopure grade, *ex.* Johnson–Matthey) centrally positioned *ca.* 50 mm apart. The foil was spot-welded to two 3 mm diameter tungsten rods and the thermocouples to 1 mm diameter tungsten rods mounted on a standard metal vacuum feedthrough. The glass reaction vessel had an optical window for pyrometer measurements protected when not in use with a magnetically operated glass shutter. The vacuum system was capable of achieving pressures below 10^{-8} Torr.

The electrical measuring and control circuit is shown in fig. 1. The specimen foil was heated with a stabilised d.c. supply (Hewlett–Packard model 6285A). The current was determined to five significant figures from the voltage drop across a standard 0.01 Ω manganin resistor using a vernier potentiometer and a digital voltmeter. The potential drop across the central uniform temperature portion of the foil was measured using the positive thermocouple leads as potential probes, to the same accuracy as the current. To eliminate the effect of the heater voltage on the thermocouple readings a reversing switch was included so that the correct value could be determined from the averaged readings. The thermocouples gave temperatures consistently low compared with the optical pyrometer because of heat conduction through the leads. They were used only to maintain uniform temperatures.

The experiments were carried out at 750 Torr pressure and a flow rate of 25 cm^3 min^{-1}. The gas supplies (grade X, B.O.C. Ltd) were purified using a platinum conversion catalyst (Engelhard M) to remove oxygen, at 723 K for methane and 298 K for hydrogen. Water and other hydrocarbon impurities were removed by passing the gas through mixed beds of 5A and 13X molecular sieves.

PROCEDURE

The iron foil was pretreated in hydrogen to remove dissolved nitrogen and surface oxide, as discussed previously,[4] except that a maximum temperature of 923 K was used so that the cold-worked layer was retained at the surface. Outgassing for *ca.* 16 h was sufficient to remove the dissolved hydrogen.[4]

Each run was started by raising the temperature with the methane flow set at the steady value. As the reaction proceeded, the heating current and voltage were adjusted to maintain a constant temperature, as measured with the pyrometer on either bright or dark surface areas. Runs were continued until localised carburisation made it difficult to maintain a uniform temperature. The region of possible 'hot spot' formation is well outside the time scale of the results presented below. If the foil was cooled during an experiment, it could not be returned to the same condition on reheating, *i.e.* to the same position on the power dissipation curve, possibly because of some irreversible graphite or carbide precipitation. Therefore, a run was normally completed without intermediate cooling.

RESULTS

The emissivity of the clean iron foil, determined from a Stefan's-law plot, has a value of 0.32, which is in good agreement with the literature value.[13] The experimental method is independent of the actual emissivity values, ε_M and ε_c, but the observed change in power dissipation increases with the difference in emissivities.

Typical power dissipation curves for the temperature range 1013-1133 K are shown in fig. 2. The absence of experimental points near $t = 0$ arises because of the carbon solution induction period. The data obey a direct logarithmic law of the type observed in some oxidation reactions,[14, 15] *i.e.*

$$\Delta W = k \log (t + t_0) - k \log (t_i + t_0) \quad (5)$$

where t_i is the induction period, and k and t_0 are constants.

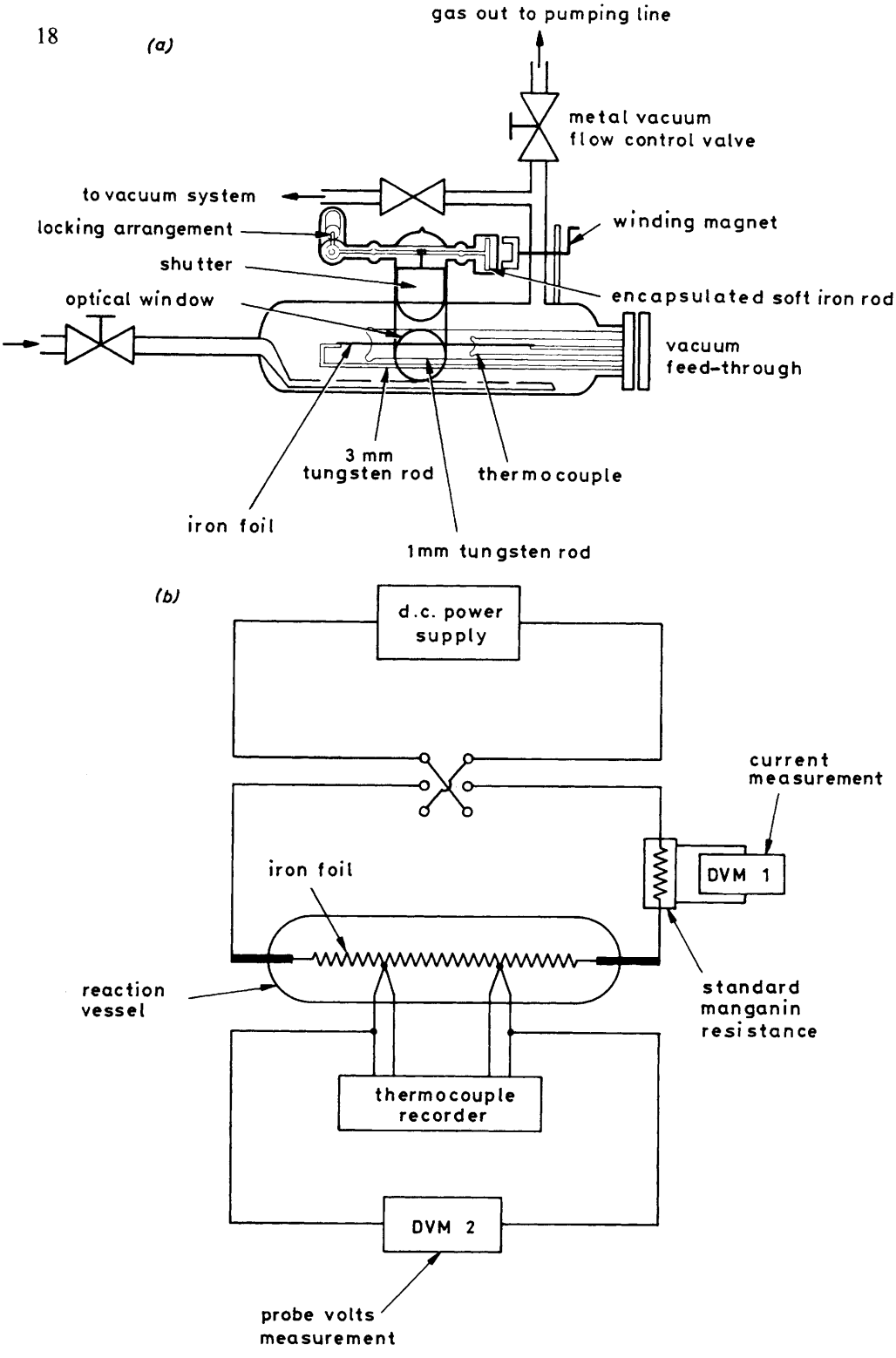

FIG. 1.—(*a*) Diagram of experimental system for resistivity/power-dissipation measurements. (*b*) Schematic diagram of the electrical circuit (DVM = digital voltmeter).

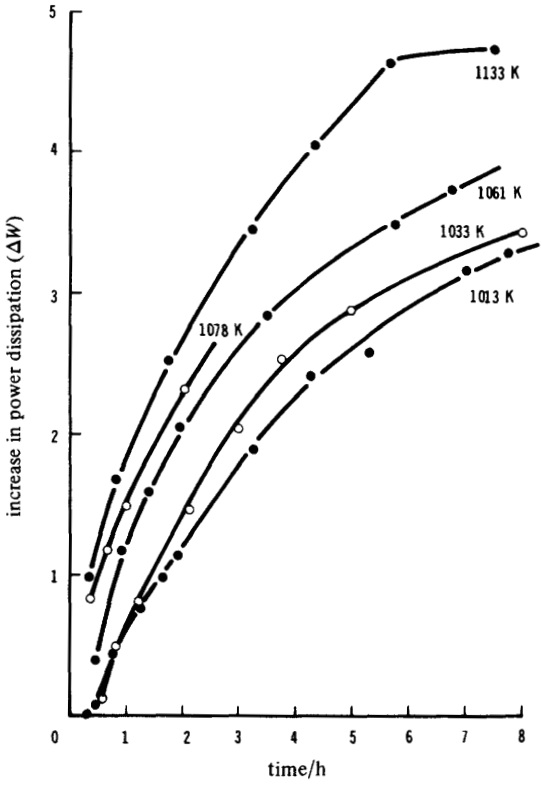

FIG. 2.—Change in power dissipation during carbon deposition from 750 Torr methane on 25 μm thick iron foils.

The data in fig. 2 are plotted in accordance with eqn (5) in fig. 3. An iterative procedure has been adopted for the determination of t_0 as follows. A plot of ΔW against log t is extrapolated back from high values of t to find the intercept value log I_1 at $\Delta W = 0$. From eqn (5), when $t \gg t_0$:

$$I_1 = t_0 + t_i. \tag{6}$$

If a new equation is written [eqn (7)]

$$\Delta W + c' = k' \log (t + I_1) \tag{7}$$

then when $\Delta W = 0$ at $t = t_i$

$$c' = k' \log (t_0 + 2t_i). \tag{8}$$

The new intercept value on the t axis is now given by

$$I_2 = t_0 + 2t_i. \tag{9}$$

Values of t_0 and t_i can be determined using eqn (6) and (9). The calculated and observed values of t_i are shown in table 1, which also lists the values of t_0 required to give linear plots. The agreement is regarded as good considering that induction periods of minutes are determined from reaction times of several hours.

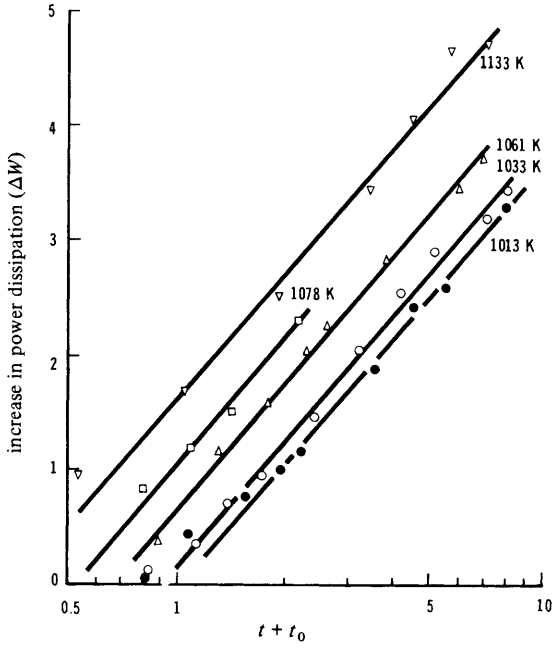

FIG. 3.—Direct logarithmic growth law plot for carbon deposition.

TABLE 1.—EXPERIMENTAL AND CALCULATED VALUES OF INDUCTION PERIOD (t_i) AND THE CONSTANT (t_0) IN S

T/K	t_i(obs)	t_i(calc)	t_0(calc)
1013	1980	2016	3204
1033	1872	1908	2844
1061	1000	720	2088
1078	720	720	1548
1133	180	216	1080

An overall activation energy for the early stage of deposit growth can be determined from values of the initial rate in fig. 3. By differentiation of eqn (5)

$$\frac{\mathrm{d}(\Delta W)}{\mathrm{d}t} = \frac{k}{t+t_0} \tag{10}$$

and therefore a plot of log (initial rate) against $1/T$, using values of t_0 from table 1 should be linear. The Arrhenius-type plot of fig. 4 gives an activation energy of 78 ± 9 kJ mol^{-1}.

The total carbon uptake into the surface layer, *i.e.* the situation that exists when the average emissivity of the foil reaches its maximum value, is given by the maximum value of $\Delta W(t)$, obtained from fig. 2 at longer times than shown. The observed values of $\Delta W(t)_{\max}$ bear a linear relationship to the reaction temperature (fig. 5). The concentration of dissolved carbon in the metal is also marked on fig. 5, the values having been determined from the γ-Fe/carbide phase boundary, which was shown

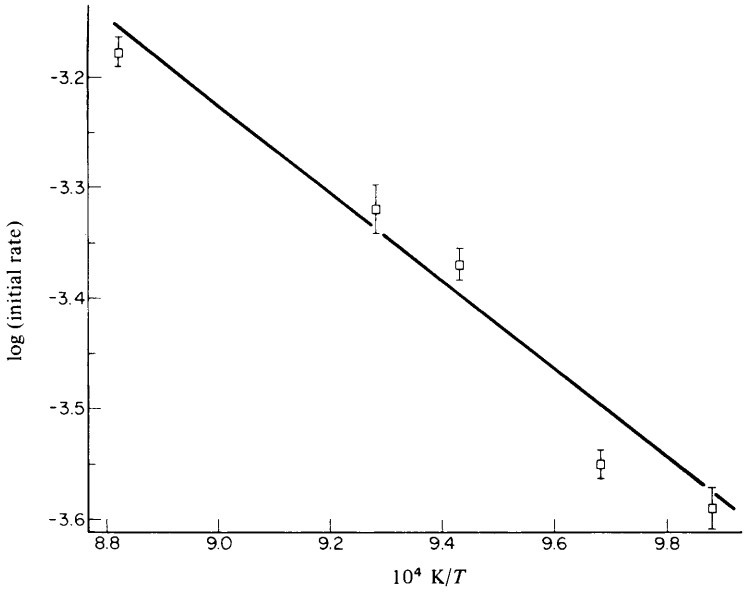

FIG. 4.—Activation energy determined from initial rate measurements. $\Delta E = 78 \pm 9$ kJ mol^{-1}.

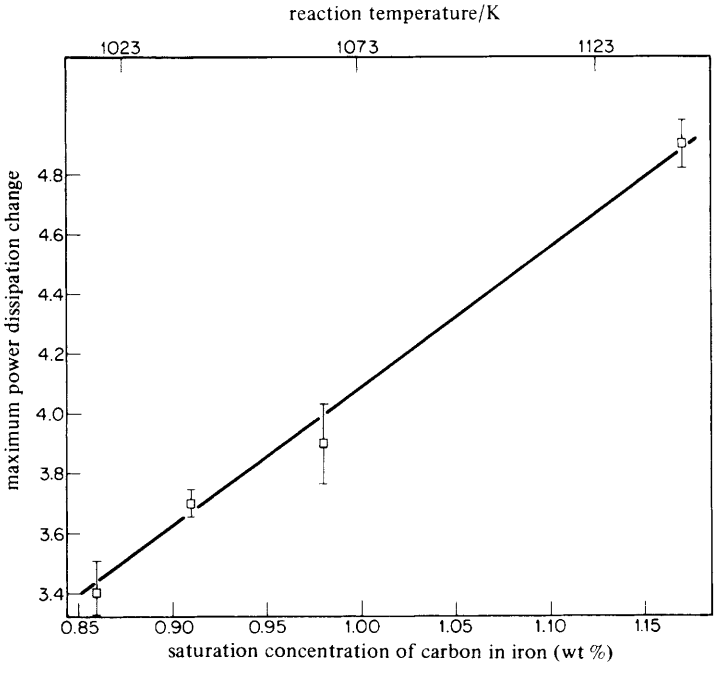

FIG. 5.—Relationship of surface coverage at maximum emissivity change to maximum dissolved carbon concentration (taken from the Fe–C phase diagram).

TABLE 2.—X-RAY ANALYSIS OF CARBON DEPOSITS

after 14 h reaction at 1033 K				after 10 h reaction at 1133 K:		data from powder diffraction file				calculated
loose deposit[a]		substrate[a]		loose deposit[a]		α-Fe (6-0696)		graphite (13-148)		γ-Fe lines[b]
d/Å	I/I_0	d/Å	I/I_0	d/Å	I/I_0	d/Å	I/I_0	d/Å	I/I_0	d/Å
3.35-3.37	100	3.36	33	3.37	100	—	—	3.35	100	—
2.13-2.14	10	2.10	17	2.12-2.13	10	—	—	2.13	50	—
2.08-2.09	10	—	—	2.08-2.09	30	—	—	—	—	2.08-2.10
				2.05	5	—	—	2.04	50	—
2.02-2.03	80	2.030	100	2.02-2.03	40	2.027	100	—	—	—
		2.025	1.7	—	—	—	—	—	—	—
		2.017	1.5	—	—	—	—	—	—	—
				1.80	10	—	—	1.80	30	1.79-1.82
				1.76-1.77	10	—	—	—	—	—
1.68-1.69	40	1.680	1.7	1.68-1.69	40	—	—	1.675	80	—
				1.58	20	—	—	1.541	60	—
1.44	10	1.430	1.2	1.43	5	1.433	19	—	—	—
				1.26-1.27	10	—	—	—	—	1.27-1.29
1.23	40	—	—	1.23	20	—	—	1.230	90	—
1.17	40	1.170	1.7	1.16-1.17	20	1.170	30	—	—	—
1.16	20	—	—	1.15-1.16	10	—	—	1.154	90	—
1.12	< 5	—	—	1.07-1.08	< 5	—	—	—	—	1.08-1.10
1.02	< 5	—	—	1.04	5	1.013	9	1.014	30	1.08-1.10
				0.993	< 5	—	—	0.991	80	—
0.907	10	0.906	1	—	—	0.906	12	—	—	0.89-0.91
						0.827	6	0.888	60	—

[a] Loose deposit examined by the Debye–Scherrer method, substrate by diffractometry; [b] γ-Fe lines calculated for concentrations in the range 1-6 atom% carbon, respectively.

to be the relevant solution limit in previous work.[12] The significance of this relationship will be discussed later.

X-ray diffraction of the deposit (removed as a powder) and of the foil (with as much loose deposit removed as possible) has been carried out using the Debye–Scherrer and diffractometry methods, respectively. The data given in table 2 show evidence of graphite, α-Fe and γ-Fe, and some weak lines that can be attributed to a carbide present in the foil, such as cementite (Fe_3C). The γ-Fe spacings are calculated from the unit-cell dimensions and the precise values are dependent on the concentration of carbon in solution.[16] The presence of γ-Fe indicates that the cooling rate on switching-off power to the filament, typically 22-25 K s^{-1}, has been sufficiently rapid to quench-in some high-temperature structure, and therefore the results provide tentative evidence for the presence of an iron carbide at temperatures above the Fe–C eutectoid. In separate high-temperature diffractometry experiments we have detected carbide lines. From X-ray measurements of the carbon interlayer spacing and using the Franklin correlation[17] it is found that 85-90% of the material has good graphitic order on the *c*-axis. Analysis of crystalline size in the *a*-axis has not been undertaken.

DISCUSSION

KINETICS

The relationship in fig. 5 implies that a fixed number of reaction sites are created at each temperature, dependent on the concentration of carbon in solution. The logarithmic growth kinetics are shown below to arise directly from the loss of active sites or active area at the surface as the reaction proceeds.

It is assumed that the decay of active sites follows an exponential law, *i.e.*

$$N(t) = N_0 \exp -k_1 \Delta W \tag{11}$$

where $N(t)$ is the number of active sites at time t, N_0 is the initial number of sites formed by the end of the induction period and k_1 is a constant. The overall rate of deposition is determined by the number of active sites available at any time t. Therefore

$$\frac{\mathrm{d}(\Delta W)}{\mathrm{d}t} = k_2 N(t). \tag{12}$$

From eqn (11) and (12) we get

$$\exp k_1(\Delta W)\,\mathrm{d}(\Delta W) = k_2 N_0\,\mathrm{d}t. \tag{13}$$

Integrating between the limits 0 to ΔW and t_i to t gives

$$[\exp k_1(\Delta W)]_0^{\Delta W} = N_0 k_1 k_2 [t]_{t_i}^{t} \tag{14}$$

i.e.

$$\exp k_1(\Delta W) = k_1 k_2 N_0 \left[t - \left(t_i - \frac{1}{k_1 k_2 N_0} \right) \right]. \tag{15}$$

If an arbitrary constant t_0 is defined such that

$$t_0 = \frac{1}{k_1 k_2 N_0} - t_i \tag{16}$$

then eqn (15) can be simplified to give

$$\exp k_1(\Delta W) = k_1 k_2 N_0 (t + t_0). \tag{17}$$

From eqn (16) and (17), taking logarithms,

$$k_1 \Delta W = \log\left(\frac{1}{t_i + t_0}\right) + \log(t + t_0) \tag{18}$$

therefore

$$\Delta W = \frac{1}{k_1}\log(t + t_0) - \frac{1}{k_1}\log(t_i + t_0). \tag{19}$$

Eqn (19) is identical to eqn (5) if $k = 1/k_1$. These constants give the value of the slope of the lines in fig. 3 and are independent of temperature.

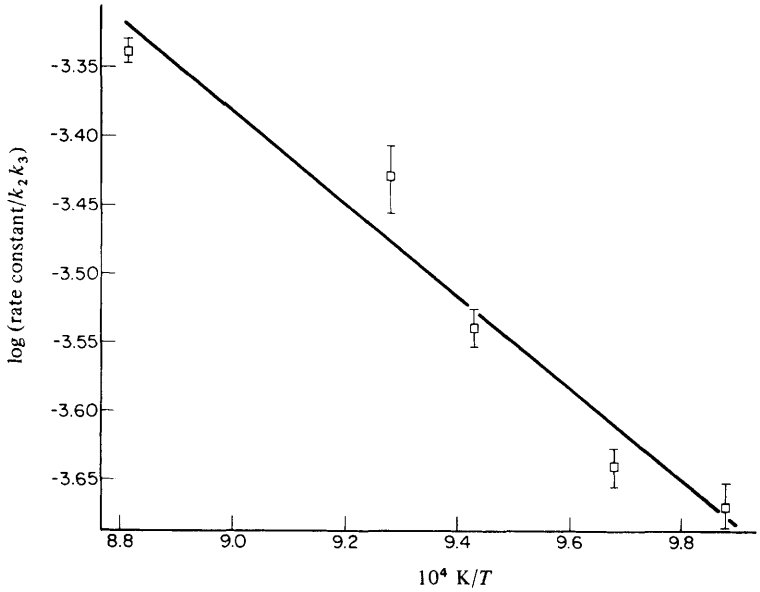

FIG. 6.—Temperature dependence of carbon depositing reaction rate constant, k_2k_3. $\Delta E = 66 \pm 8$ kJ mol^{-1}.

The temperature dependence of k_2 gives the true activation energy of the deposition process. It can be derived from eqn (16) using the appropriate temperature-dependent values of N_0. From fig. 5 it can be seen that

$$N_0 = k_3(aT + b) \tag{20}$$

where k_3, a and b are constants, the latter two being obtained directly from the figure. From eqn (16) and (20) we have

$$k_2 k_3 = \frac{1}{k_1(t_i + t_0)(aT + b)}. \tag{21}$$

The constant k_3 converts ΔW_{max} and temperature data from fig. 5 into numbers of sites, and its absolute value is not known. However, the true activation energy can be obtained by plotting log (k_2k_3) obtained from eqn (21) against $1/T$, as in fig. 6, which gives a value of 66 ± 8 kJ mol^{-1}.

The calculation based on eqn (21) would give the same activation energy as that using eqn (10) if N_0 were independent of temperature, which occurs only in the

eutectoid region of the Fe–C phase diagram, *i.e.* $T = 996$ or 1011 K. The use of initial rates to derive an activation energy is only justified when there is insufficient information about the reaction mechanism. With a specimen in the form of a thin foil, the solution and initial surface deposition stages are separated in time because a homogeneous solid solution of carbon in the metal can be formed rapidly. With a thicker bulk specimen some deposition may occur at the surface before a saturated solution is formed in the centre, for example because easy diffusion paths have been blocked. In these circumstances a detailed analysis of the kinetics on the above scheme would be difficult as extra terms would be required to account for diffusion, precipitation and possible break-up of the metal structure in the surface zone. Therefore, only rate data taken at the earliest time that surface deposits were detectable could be used to make a meaningful comparison with the thin foil data.

RATE-DETERMINING STEP

The kinetic analysis above does not allow the rate-determining step to be distinguished. The activation energy of 66 kJ mol^{-1} is too low for carbon dissolution in γ-Fe rate control, for which $E = 190$ kJ mol^{-1}.[12] In the temperature range 1013-1133 K the carbon solubility at the γ-Fe (austenite) phase boundary is 3.9-4.4 atom% C, respectively.[18] The activation energy for diffusion in γ-Fe is a function of carbon content, and literature data[19,20] for this concentration range give values of 130-134 kJ mol^{-1}, respectively. Enthalpies of solution for carbon in γ-Fe of 40.6 kJ mol^{-1} [21] and 44.7 kJ mol^{-1} [22] have been reported, and therefore if either value is added to the activation energy of diffusion to obtain a calculated total energy change, then an activation energy of 170-179 kJ mol^{-1} could have been observed.

In situ SEM studies have shown that below the Fe–C eutectoid temperature (996 or 1011 K) carbon precipitation is accompanied by reorganisation of the metal surface,[23] and therefore it is probable that similar mass-transfer processes will occur above the eutectoid temperature, in which case self-diffusion of iron atoms could be rate-determining. However, surface self-diffusion and bulk self-diffusion in γ-Fe have an activation energy in excess of 200 kJ mol^{-1} [24] and of 280 kJ mol^{-1},[25] respectively. Therefore surface and bulk diffusion of iron atoms, as well as carbon dissolution and carbon diffusion through the bulk metal, can be eliminated as possible rate-determining steps.

There are a few studies in the literature in which the kinetics of clearly identifiable single carbon morphologies have been measured. The rate of carbon filament growth on iron particles is reported to have an activation energy of 67.3 kJ mol^{-1} in the temperature range 925-1245 K, *i.e.* both below and above the eutectoid, rate control being attributed to bulk diffusion through the metal.[3] This value is less than the activation energy for diffusion of carbon in α-Fe, *i.e.* 84-105 kJ mol^{-1},[20] or in γ-Fe (see above). Although the same rate-controlling step may apply to both monticular and filamentary growth, there is no evidence that it is dependent on the diffusion of carbon through the bulk metal in the case of iron.

An activation energy of 66.9 kJ mol^{-1} has been reported for the growth of laminar carbon films above 653 K on nickel from butadiene and propene, and on iron from butadiene.[26] The similarity of the activation energy for the development of different morphologies for a variety of gas–metal systems suggests that the same rate-controlling step may apply. This could be surface diffusion of carbon atoms or metal–carbon–hydrogen species on the metal as suggested previously,[26] or mobility of catalytic metal species at the carbon–metal interface. High mobilities of metal particles on graphite surfaces have been observed in microscopic studies of graphite oxidation.[27,28]

The correlation of the maximum island area of carbon formed at each temperature

with the amount of carbon in the saturated solution, fig. 5, implies that a fixed number of nucleation sites are created from the dissolved carbon. Dissolution of an evaporated carbon layer on nickel by high-temperature annealing followed by reprecipitation was also found to create sites for subsequent deposition from acetylene.[29]

The carbon that is precipitated in the monticular growths prevents further gas attack of the metal in these areas. The lateral growth of the carbon mounds ceases before the metal surface is fully covered. Subsequent reaction occurs between the mounds, a particulate type of carbon deposit being formed.[5]

Part of this work was carried out as a Ph.D. programme (A.M.E.) with the University of Edinburgh. We thank Prof. C. Kemball for his assistance in making the arrangement, and Dr D. Taylor for helpful discussions. The work was carried out at the Central Electricity Research Laboratories and is published by permission of the Central Electricity Generating Board.

[1] A. M. Brown, A. M. Emsley and M. P. Hill, in *Gas Chemistry in Nuclear Reactors and Large Industrial Plant*, ed. A. Dyer (Heydon, London 1980), p. 26.
[2] S. D. Robertson, *Carbon*, 1970, **3**, 365; 1972, **10**, 221.
[3] R. T. K. Baker, P. S. Harris, R. B. Thomas and R. J. Waite, *J. Catal.*, 1973, **30**, 86.
[4] A. M. Emsley and M. P. Hill, *Carbon*, 1977, **15**, 205.
[5] A. M. Brown and M. P. Hill, *Proc. 3rd Int. Carbon Conf.* (Deutschen Keramischen Gesellschaft, Baden-Baden, 1980), p. 21.
[6] G. Blau and A. E. B. Presland, *3rd Conf. on Industrial Carbon and Graphites* (Society of Chemical Industry, London 1970).
[7] R. T. K. Baker, P. S. Harris, J. Henderson and R. B. Thomas, *Carbon*, 1975, **13**, 17.
[8] F. J. Derbyshire, A. E. B. Presland and D. L. Trimm, *Carbon*, 1975, **13**, 189.
[9] S. M. Irving and P. L. Walker Jr, *Carbon*, 1967, **5**, 399.
[10] T. Baird, *Carbon*, 1977, **15**, 379.
[11] R. T. K. Baker, *Chemistry and Physics of Carbon*, ed. P. L. Walker Jr and P. A. Thrower (Marcel Dekker, New York, 1978), vol. 14, p. 83.
[12] A. M. Emsley and M. P. Hill, *J. Chem. Soc., Faraday Trans. 1*, 1983, **79**, 1.
[13] *Handbook of Chemistry and Physics*, ed. C. R. Weast (C.R.C. Press, Cleveland, Ohio, 59th edn, 1978-9), p. E364.
[14] U. R. Evans, *The Corrosion and Oxidation of Metals* (Arnold, London, 1960).
[15] K. R. Lawless, *Rep. Prog. Phys.*, 1974, **37**, 231.
[16] A. Taylor, *X-ray Metallography* (Wiley, New York, 1961), p. 524.
[17] R. E. Franklin, *Acta Crystallogr.*, 1951, **4**, 253.
[18] H. Goldschmidt, *Interstitial Alloys* (Butterworths, London, 1967).
[19] C. Wells, W. Baty and R. F. Mehl, *Trans. AIME*, 1950, **188**, 553.
[20] J. D. Fast, *Interaction of Metals and Gases* (Macmillan, London, 1971), vol. 2.
[21] J. A. Lobo and G. H. Geiger, *Metall. Trans.*, 1976, **7A**, 1359.
[22] J. Chipman, *Trans. Metall. Soc. AIME*, 1967, 239.
[23] A. M. Brown and M. P. Hill, *Carbon*, 1981, **19**, 51.
[24] G. Neumann and G. M. Neumann, *Surface Self-Diffusion of Metals, Diffusion Monograph Ser. No. 1* (Diffusion Information Centre, Solothurn, Switzerland).
[25] *Handbook of Chemistry and Physics*, ed. C. R. Weast (C.R.C. Press, Cleveland, Ohio, 59th edn, 1978-9), p. F65.
[26] T. Baird, in *Gas Chemistry in Nuclear Reactors and Large Industrial Plant*, ed. A. Dyer (Heydon, London, 1980), p. 35.
[27] J. M. Thomas, in *Chemistry and Physics of Carbon*, ed. P. L. Walker Jr (Dekker, New York, 1965), vol. 1, p. 121.
[28] G. R. Hennig, in *Chemistry and Physics of Carbon*, ed. P. L. Walker Jr (Marcel Dekker, New York, 1966), vol. 2, p. 1.
[29] C. Bernardo and L. S. Lobo, *Carbon*, 1976, **14**, 287.

(PAPER 1/1502)